

Supplementary Information

Ni₃S₂/Cu-NiCo LDH Heterostructure Nanosheet Array on Ni Foam for Electrocatalytic Overall Water Splitting

Lina Jia,^{1,2} Gaohui Du,^{1,*} Di Han,^{1,2} Yawen Hao,^{1,2} Wenqi Zhao,¹ Yi Fan,^{1,2}

Qingmei Su,^{1,*} Shukai Ding,¹ Bingshe Xu¹

*Corresponding author: Email: dugaohui@sust.edu.cn; suqingmei@sust.edu.cn

¹ Materials Institute of Atomic and Molecular Science, Shaanxi University of Science and Technology, Xi'an, 710021, China.

² School of Materials Science & Engineering, Shaanxi University of Science and Technology, Xi'an, 710021, China.

Characterization

The D/max2200PC X-ray diffractometer with Cu K α radiation ($\lambda=1.5418$ Å) was utilized to detect the crystal phase of the materials. Scanning electron microscopy (SEM, HITACHI SU5000) and transmission electron microscopy (TEM, ARM 300F) was utilized to confirm the morphology and microstructure. The electron energy loss spectroscopy (EELS) elemental mapping was recorded using a Gatan Imaging Filter (GIF) spectrometer attached to the TEM (ARM 300F). X-ray photoelectron spectra (XPS) on a Thermo Fisher K-Alpha Spectrometer was employed to ascertain the chemical composition of the materials. Inductively coupled plasma optical emission spectroscopy (ICP-OES; Agilent 5110) was used to analyze the chemical composition.

Electrochemical Measurement

The HER and OER performance was tested in 1 M KOH solution with the three-electrode system using CHI 660C electrochemical workstation at room temperature. The Ni foam supported active materials with a geometric area of 1×1 cm was immersed into the solution as the working electrode. The loading mass of Ni₃S₂/Cu-NiCo LDH on the NF is 1.74 mg cm⁻². A standard Ag/AgCl electrode and a graphite rod were served as the reference and counter electrodes, respectively. For comparison, the mass loading of IrO₂ and Pt/C (Pt loading: 20 wt.%) catalysts on NF is 1.74 mg

cm⁻², which is the same amount with Ni₃S₂/Cu-NiCo LDH on NF. In a typical preparation procedure, a homogeneous catalyst solution with 4.0 mg of commercial IrO₂ or Pt/C, 736 μL deionized water, 184 μL of ethanol and 80 μL of Nafion solutions (5%) was prepared by sonicating for 30 min. Subsequently, 435 μL of the catalyst solution was drop-cast onto a piece of clean NF (1 cm × 1 cm), and the prepared electrode was dried at 60 °C before electrochemical measurements.

Before HER and OER activity test, 1 M KOH electrolyte was saturated with N₂ and O₂ for at least 30 min to mitigate dissolved oxygen and ensure the O₂ saturation, respectively. Prior to LSV test, the working electrode were pre-activated by 20 cycles of cyclic voltammetry (CV) scan. The potential ranges are from -1 V to -1.3 V (*vs.* Ag/AgCl) for HER and from 0.2 V to 0.4 V (*vs.* Ag/AgCl) for OER, respectively. The electrochemical impedance spectrum (EIS) test of the catalysts were carried out with a frequency range of 1 Hz to 10 kHz at the overpotential corresponding to the current density of 100 mA cm⁻². To evaluate the activity of the obtain samples, the linear sweep voltammetry (LSV) was performed between -0.9 V and -1.6 V (*vs.* Ag/AgCl) for HER, 0 and 1 V (*vs.* Ag/AgCl) for OER at 5 mV s⁻¹, respectively. All the LSV tests were performed with 90% iR compensation, in which the resistances are about 1.8 – 1.9 Ω for OER, 1.7 – 1.8 Ω for HER, and 4 – 5 Ω for overall water-splitting, respectively. The electrochemical surface area (ESCA) was estimated from the double-layer capacitance (C_{dl}) of the electrocatalyst materials. The C_{dl} was determined by a simple CV method. The CV was conducted at various scan rates of 10, 20, 30, 50, 70, and 100 mV s⁻¹. The long-term durability tests were executed using the chronoamperometry method under the constant potential of 0.39 V (*vs.* Ag/AgCl) for OER and -1.35 V (*vs.* Ag/AgCl) for HER, which corresponds to the current density of 100 mA cm⁻².

Overall water splitting performance tests were performed using CHI 660C electrochemical workstation with the Ni₃S₂/Cu-NiCo LDH/NF as both the cathode and anode. LSV measurement was carried out in 1 M KOH solution with a scan rate of 5 mV s⁻¹. The overall water splitting stability of the obtained samples was measured by chronoamperometry for 12 h at a constant potential of 1.75 V corresponding to the current density of 100 mA cm⁻².

The potential *versus* the reversible hydrogen electrode (*vs.* RHE) was calculated by adding 1.046 V in 1 M KOH according to the equation: $E_{RHE} = 0.22 V + 0.059 \times pH + E_{Ag/AgCl}$.

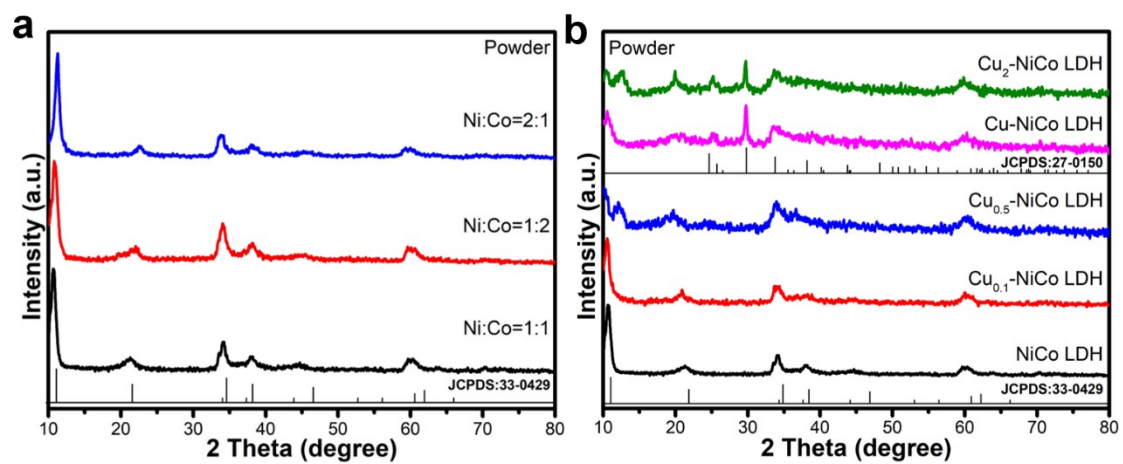


Figure S1. XRD patterns of (a) Ni: Co molar ratio of 1:1, 1:2, 2:1, and (b) Ni: Co: Cu molar ratio of 1:1:0, 1:1:0.1; 1:1:0.5, 1:1:1, 1:1:2.

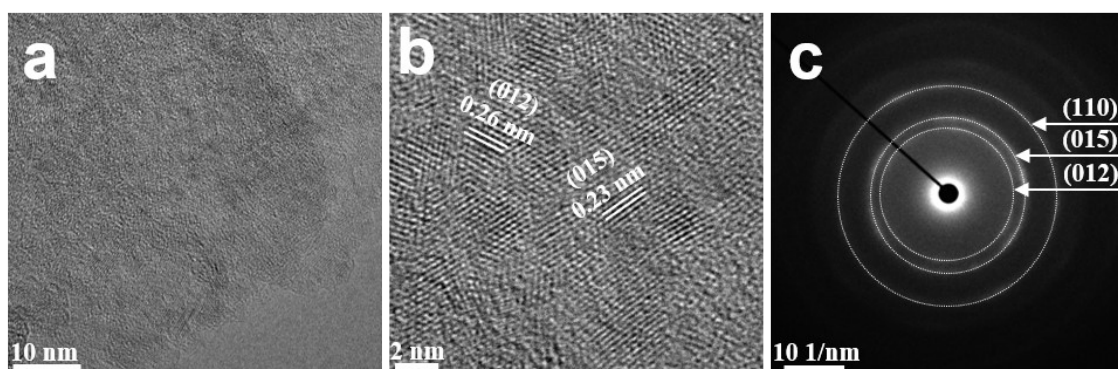


Figure S2. (a) TEM image, (b) HRTEM image, and (c) SAED pattern of NiCo LDH/NF.

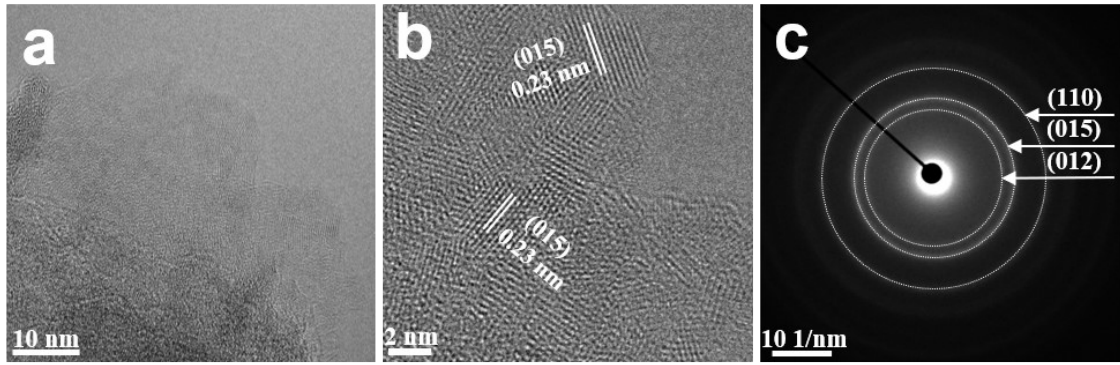


Figure S3. (a) TEM image, (b) HRTEM image, and (c) SAED pattern of Cu-NiCo LDH/NF.

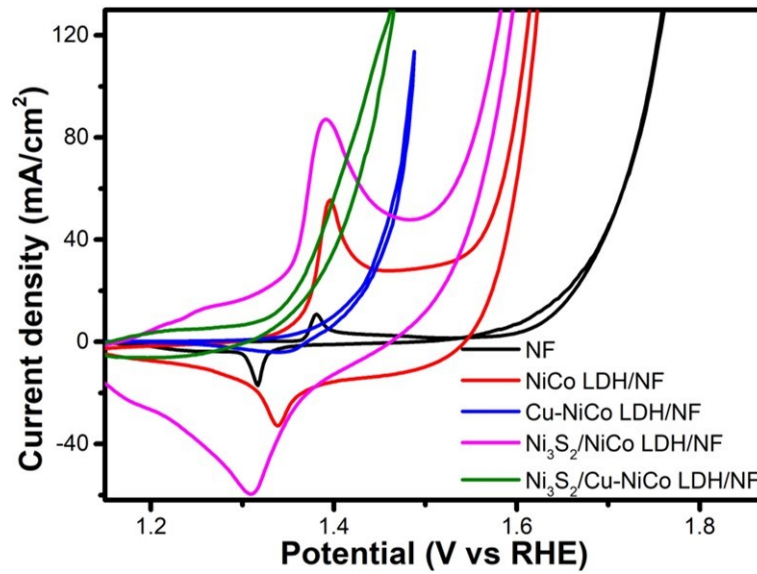


Figure S4. Cyclic voltammograms (CV) of $\text{Ni}_3\text{S}_2/\text{Cu-NiCo LDH/NF}$, $\text{Ni}_3\text{S}_2/\text{NiCo LDH/NF}$, Cu-NiCo LDH/NF , NiCo LDH/NF and NF with a scan rate of 5 mV/s in a 1 M KOH solution.

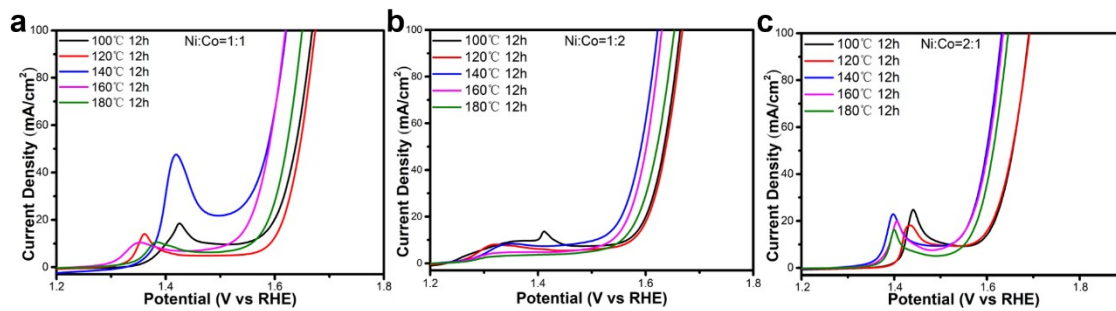


Figure S5. OER polarization curves of NiCo LDH/NF with Ni and Co molar ratios of 1:1, 1:2 and 2:1 at different hydrothermal temperatures.

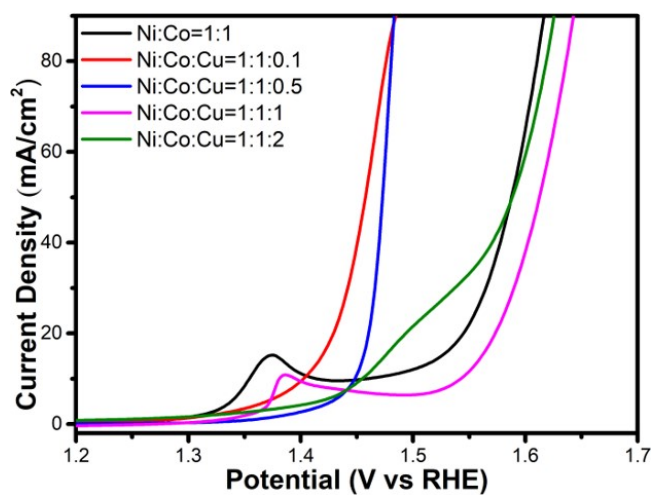


Figure S6. OER polarization curves of Cu-NiCo LDH/NF with different Cu doping (0.1, 0.5, 1, 2 mmol) at 140 °C for 12 h (Ni:Co=1:1).

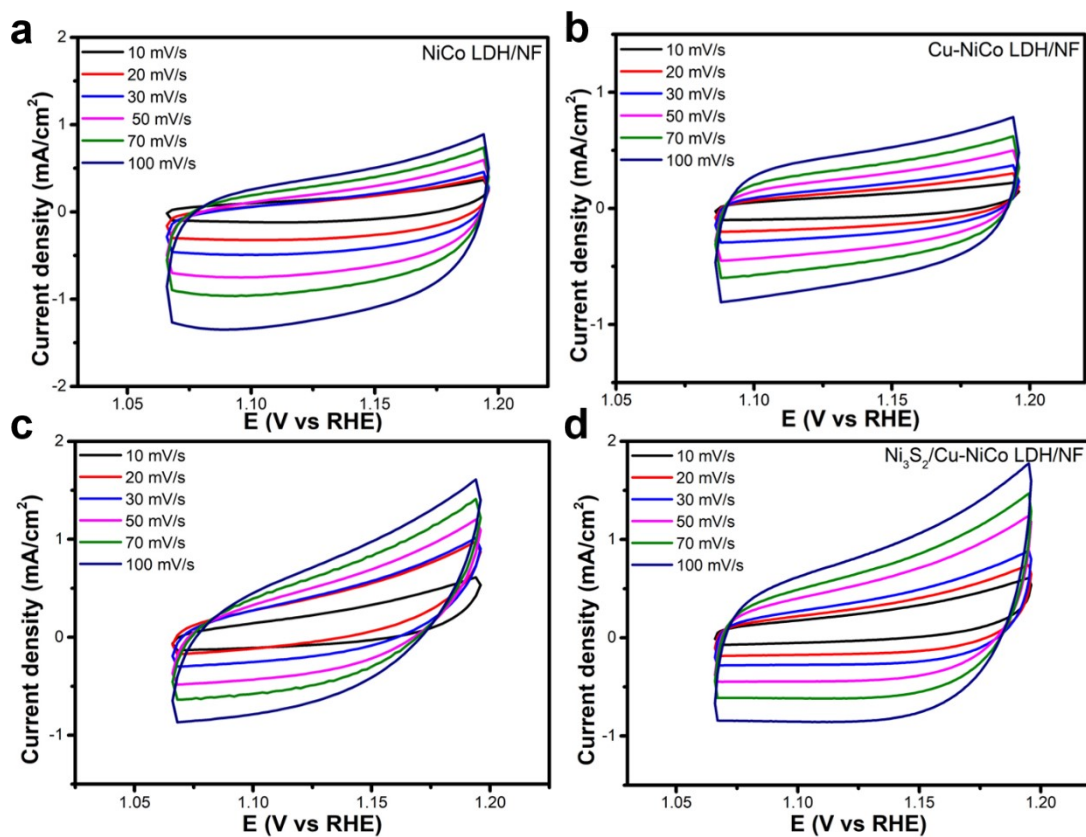


Figure S7. The electrochemically effective surface area of (a) NiCo LDH/NF, (b) Cu-NiCo LDH/NF, and (c) Ni₃S₂/Cu-NiCo LDH/NF in OER.

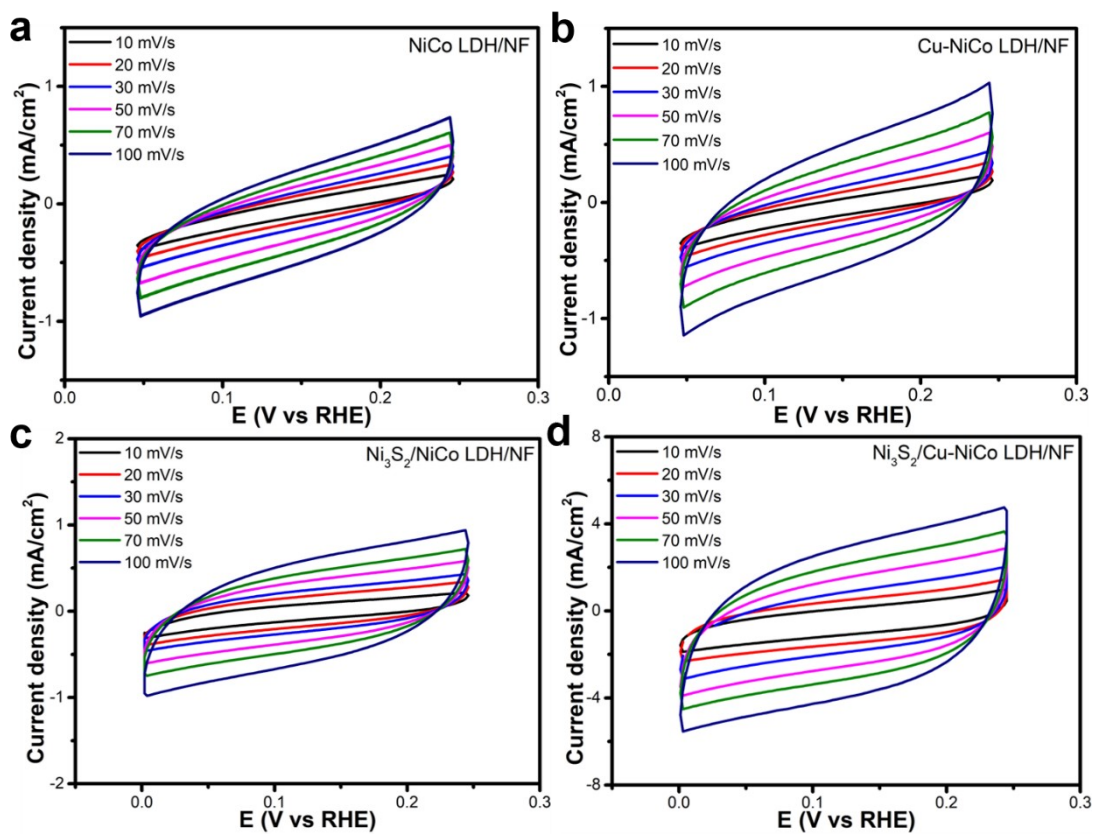


Figure S8. The electrochemically effective surface area of (a) NiCo LDH/NF, (b) Cu-NiCo LDH/NF, (c) Ni₃S₂/Cu-NiCo LDH/NF in HER.

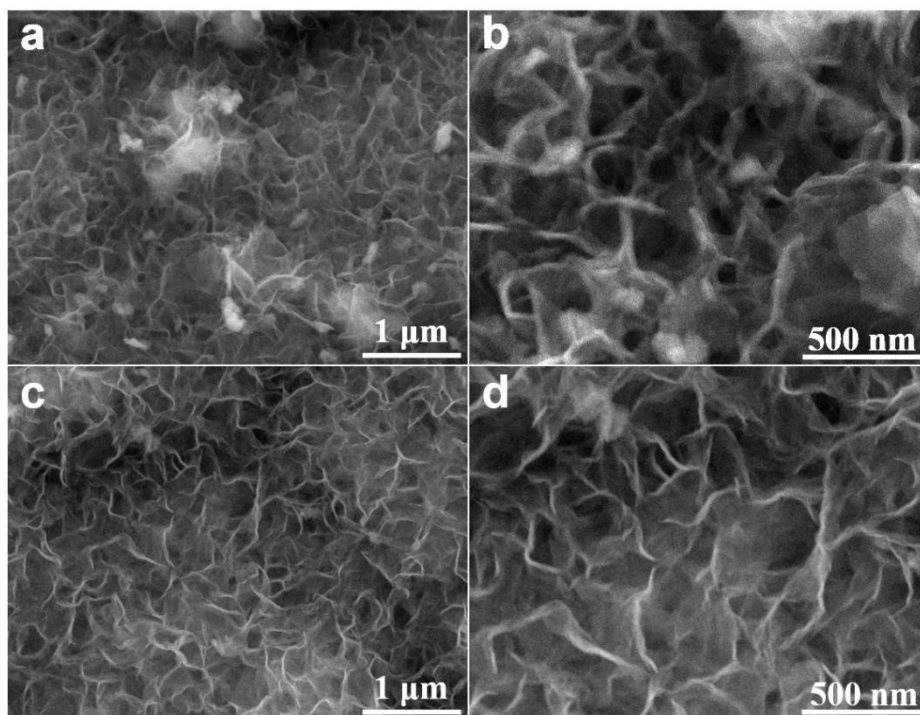


Figure S9. SEM images of $\text{Ni}_3\text{S}_2/\text{Cu-NiCo LDH/NF}$ samples after HER (a, b) and OER (c,d) tests.

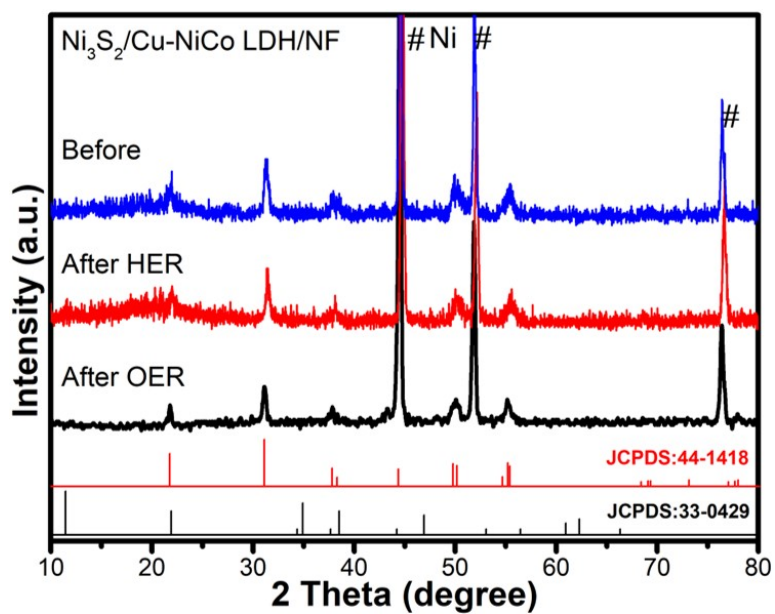


Figure S10. XRD patterns of $\text{Ni}_3\text{S}_2/\text{Cu-NiCo LDH/NF}$ samples before and after HER and OER tests.

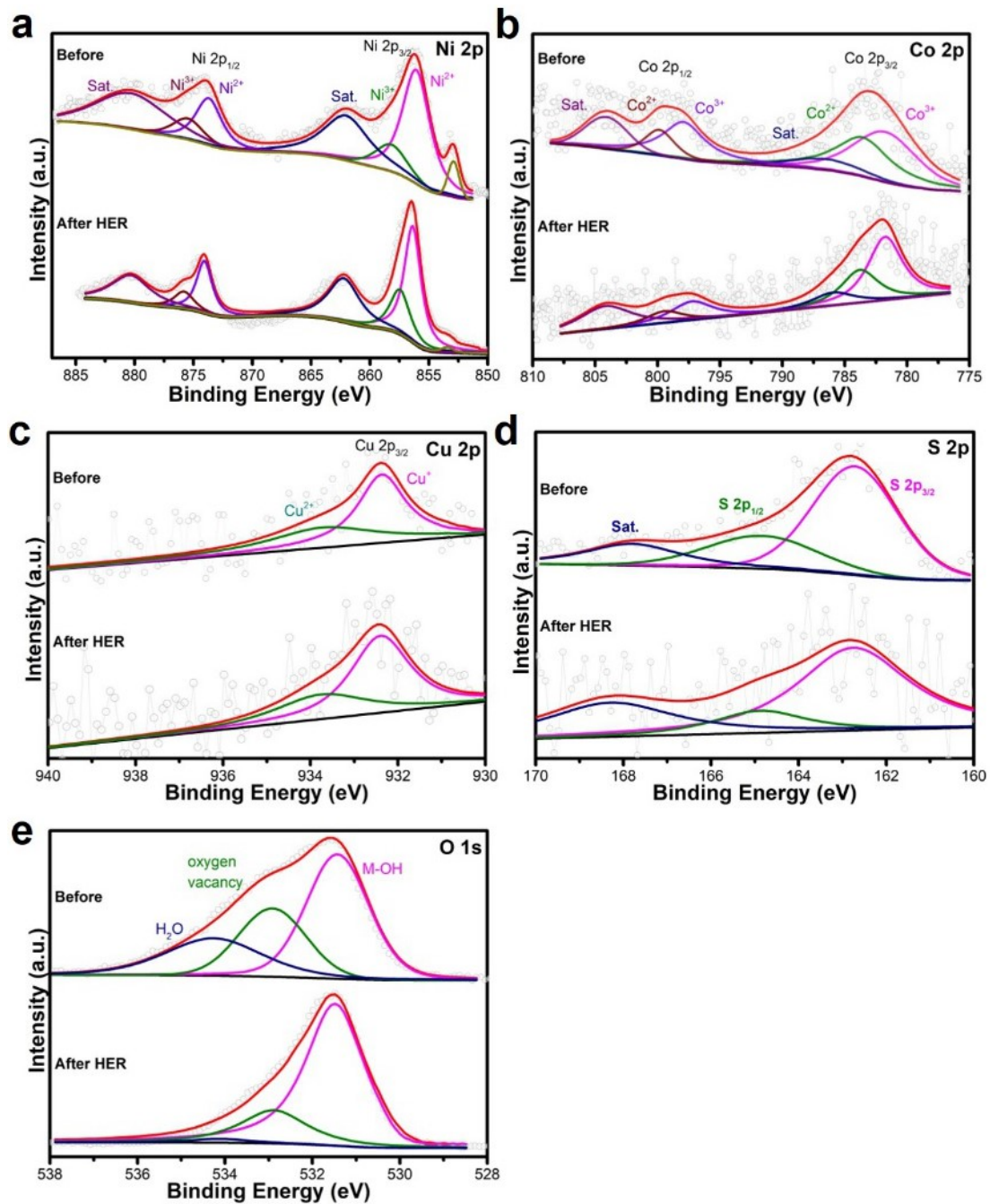


Figure S11. High resolution XPS spectra of (a) Ni 2p, (b) Co 2p, (c) Cu 2p, (d) S 2p and (e) O 1s of Ni₃S₂/Cu-NiCo LDH/NF before and after HER test.

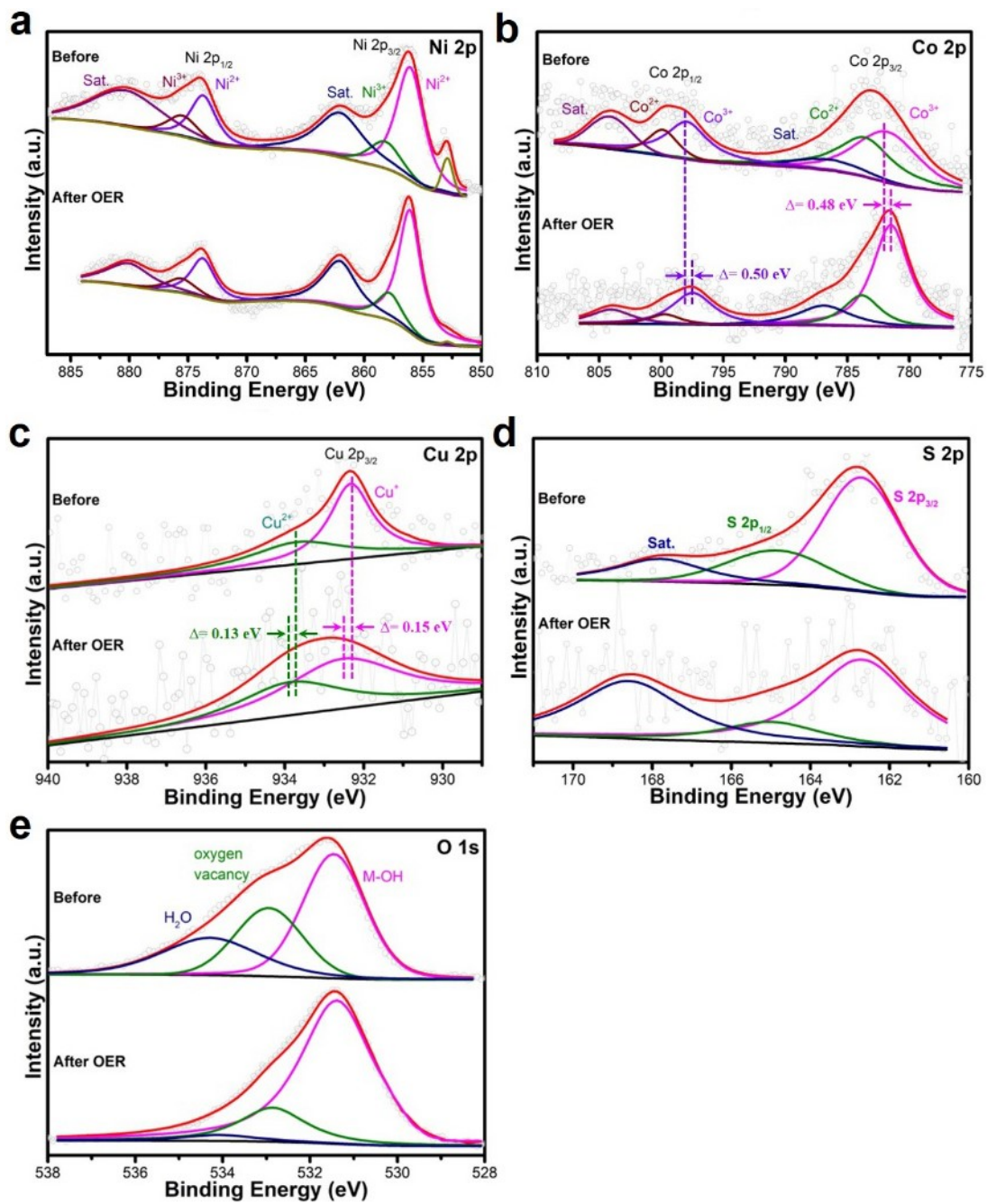


Figure S12. High resolution XPS spectra of (a) Ni 2p, (b) Co 2p, (c) Cu 2p, (d) S 2p and (e) O 1s of $\text{Ni}_3\text{S}_2/\text{Cu-NiCo LDH}/\text{NF}$ before and after OER test.

Table S1. Comparison of OER performance of similar materials in alkaline media.

Catalyst	Overpotential (η_{10}) (mV)	η_{100} (mV)	Tafel (mV dec ⁻¹)	Electrolyte	Ref.
Ni ₃ S ₂ /Cu-NiCo LDH/NF	119	218	70	1.0 M KOH	This Work
NiCo ₂ S ₄ NW/NF	260	380	40.1	1.0 M KOH	1
PA-ZnFeCo LDH/NF	221	276	58.73	1.0 M KOH	2
Ni _{0.75} Fe _{0.125} V _{0.125} - LDHs/NF	231	255	39.4	1.0 M KOH	3
CoMoV LDH/NF	270	450	106	1.0 M KOH	4
CoFe@NiFe/NF	190	255	45.71	1.0 M KOH	5
S-NiCoFe LDH/CC	206	258	46	1.0 M KOH	6
NiCo ₂ S ₄ @CoNi- LDH/CC	-	337	111.2	1.0 M KOH	7
np-NiAl-LDH/NF	-	314	93	1.0 M KOH	8

Table S2. Comparison of HER performance with other similar materials in alkaline media.

Catalyst	Overpotential (η_{10}) (mV)	η_{100} (mV)	Tafel (mV dec ⁻¹)	Electrolyte	Ref.
Ni ₃ S ₂ /Cu-NiCo LDH/NF	156	304	129	1.0 M KOH	This Work
NiCo ₂ S ₄ NW/NF	210	350	58.9	1.0 M KOH	1
CoMoV LDH/NF	150	360	182	1.0 M KOH	4
CoFe@NiFe/NF	240	335	88.88	1.0 M KOH	5

Table S3. Comparison of overall water splitting performance with other similar materials in alkaline media.

Catalyst	Potential (at 10 mA cm ⁻²) (V)	Potential (at 100 mA cm ⁻²) (V)	Electrolyte	Ref.
Ni ₃ S ₂ /Cu-NiCo LDH/NF	1.58	1.75	1.0 M KOH	This Work
NiCo ₂ S ₄ NW/NF	1.63	-	1.0 M KOH	1
Ni _{0.75} Fe _{0.125} V _{0.125} - LDHs/NF	1.591	1.83	1.0 M KOH	3
CoMoV LDH/NF	1.61	2.01	1.0 M KOH	4
CoFe@NiFe/NF	1.59	-	1.0 M KOH	5
np-NiAl-LDH/NF	1.44	1.75	1.0 M KOH	8

References

- [1] A. Sivanantham, P. Ganesan and S. Shanmugam, *Adv. Funct. Mater.*, 2016, **26**, 4661-4672.
- [2] J. X. Han, J. Zhang, T. T. Wang, Q. Xiong, W. Wang, L. X. Cao and B. H. Dong, *ACS Sustain. Chem. Eng.*, 2019, **7**, 13105-13114.
- [3] K. N. Dinh, P. L. Zheng, Z. F. Dai, Y. Zhang, R. Dangol, Y. Zheng, B. Li, Y. Zong and Q. Y. Yan, *Small*, 2018, **14**, 4724.
- [4] J. Bao, Z. L. Wang, J. F. Xie, L. Xu, F. C. Lei, M. L. Guan, Y. Zhao, Y. P. Huang and H. M. Li, *ChemComm*, 2019, **55**, 3521-3524.
- [5] R. Yang, Y. M. Zhou, Y. Y. Xing, D. Li, D. L. Jiang, M. Chen, W. D. Shi and S. Q. Yuan, *Appl. Catal. B*, 2019, **253**, 131-139.
- [6] L. M. Cao, J. W. Wang, D. C. Zhong and T. B. Lu, *J. Mater. Chem. A*, 2018, **6**, 3224-3230.
- [7] F. F. Yuan, J. D. Wei, G. X. Qin and Y. H. Ni, *J. Alloys Compd.*, 2020, **830**, 154658.
- [8] L. L. Feng, Y. Y. Du, J. F. Huang, L. Y. Cao, Q. Q. Liu, D. Yang and K. Kajiyoshi, *Sustainable Energy Fuels*, 2020, **4**, 2850-2858.